Chemical Science

EDGE ARTICLE

View Article Online
View Journal | View Issue

Check for updates

Cite this: *Chem. Sci.*, 2019, **10**, 2206

All publication charges for this article have been paid for by the Royal Society of Chemistry

Received 22nd October 2018
Accepted 17th December 2018

DOI: 10.1039/c8sc04701d

rsc.li/chemical-science

Enhanced optomechanical properties of mechanochemiluminescent poly(methyl acrylate) composites with granulated fluorescent conjugated microporous polymer fillers†

Yuan Yuan,[ab] Weiben Chen,[ab] Zhe Ma,[c] Yakui Deng,[ab] Ying Chen,[ab] Yulan Chen *[ab] and Wenping Hu *[ab]

With the combination of mechanochemiluminescence from 1,2-dioxetane coupled polymers and granulated conjugated microporous polymer (CMP) nanosheets, a new kind of filling-type mechanolumninescent polymer composite was developed. Herein, polymeric 1,2-dioxetane performed as an autoluminescent probe of chain scission. Besides benefiting from their excellent optical properties and good interfacial compatibility with poly(methyl acrylate) (PMA) media, two stable and fluorescent CMP nanosheets were prepared and dispersed in crosslinked PMA, which can serve as effective energy acceptors and reinforcing nano-fillers. These polymer nanocomposites present both reinforced mechanical strength and mechanochemiluminescence, and offer exciting opportunities to study the failure process of polymer nanocomposites with unprecedented temporal and spatial resolution.

Introduction

Filling-type polymer nanocomposites have attracted significant attention since they could effectively modulate the mechanical properties of the as-obtained materials, leading to optimal performance and new functions.[1–5] Traditional filling particles, such as silica, carbon black, montmorillonite, *etc.* could improve the fracture strength and the modulus of the composites. Nevertheless, the development of these polymeric nanocomposites has been frustrated by difficulties in the dispersion of these nano-fillers into polymer media, mainly deriving from their poor surface adhesion/cohesion with a hydrophobic polymer matrix and the need for severe preparation conditions. Another great challenge in inorganic/polymer composites is the efficient translation of inorganic filler properties into the polymer matrix. Recent works concerning covalent organic polymer (COP) nanosheets or nanoparticles obtained from bulk COPs through a "top-down" strategy[6–11] indicated that these nanosized COPs could act as polymer fillers with good interactions with the polymer matrix.[12–14] By virtue of their structural tunability and rich functionality with intrinsic polymer characteristics, COP network based fillers possess great advantages over conventional inorganic counterparts. We thus envisioned that with doping of granulated COPs,[15,16] particularly fluorescent conjugated microporous polymers (CMPs), the mechanical strength or toughness of polymer composites could be enhanced with integrated new functions, such as abrasion, tunable optical properties, *etc.*

Polymer mechanochemistry, whereby chemical transformations in polymers are facilitated using mechanical force, is becoming a burgeoning area, and mechano-active polymers have boosted the development of stress sensing materials through the translation of macroscopic force into specific outputs.[17,18] Mechanochemiluminescent polymers, considered to be among the most sensitive stress sensing materials, were first reported by Sijbesma,[19] using 1,2-dioxetane as the mechanophore. When bis(adamantyl)-1,2-dioxetane was covalently functionalized with polymer chains, the transduction of mechanical force along the polymer backbone to the strategically weakened O–O bonds led to the local dissociation of the dioxetane ring. Two ketones were thus generated, one of which was in the excited state and emits a photon upon relaxation, exhibiting transient blue autoluminescence (Scheme 1A). This process constitutes a novel way to probe mechanochemical chain scission with high resolution in space and time, and has the capability to provide exceptionally detailed insight into the

[a]*Tianjin Key Laboratory of Molecular Optoelectronic Science, Department of Chemistry, Tianjin University, Tianjin 300354, P. R. China. E-mail: yulan.chen@tju.edu.cn; huwp@tju.edu.cn*

[b]*Collaborative Innovation Centre of Chemical Science and Engineering, Tianjin 300072, P. R. China*

[c]*School of Materials Science and Engineering, Tianjin University, Tianjin 300354, P. R. China*

† Electronic supplementary information (ESI) available: Experimental procedures, characterization data for granulated CMPs, CMP/PMA composites, optomechanical test results of CMP/PMA and mechanochemiluminescent videos of CMP/PMA films during stretching. See DOI: 10.1039/c8sc04701d

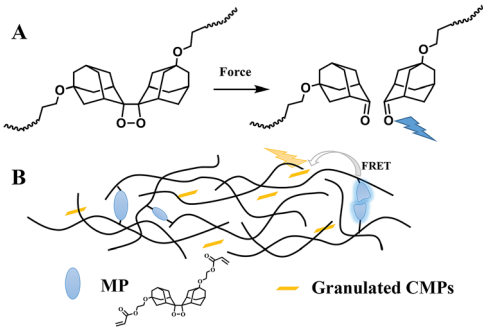

Scheme 1 (A) Schematic of mechanically induced chemiluminescence from a polymeric bis(adamantyl)-1,2-dioxetane. (B) Schematic of mechanochemiluminescent CMP/PMA composites.

origins and mechanisms of failure in polymeric materials. To increase the sensitivity, fluorescent dyes were physically mixed in the polymer films an energy acceptors to enhance the light intensity.

Introducing the 1,2-dioxetane probe in appropriate materials platforms, such as polymer melts, gels, or thermoplastic elastomers, not only promises widespread application in studying mechanical phenomena in polymeric materials, but also achieves great progress in the development of advanced responsive materials.[20–24] Despite the prevalent utilities of polymer nanocomposites with their complex fracture mechanisms, until now, the mechanochemiluminescent feature has rarely been investigated in polymer nanocomposites, especially with organic nano-fillers. In this work, we prepared two kinds of mechanochemiluminescent composites of fluorescent CMPs[25] dispersed in poly(methyl acrylate) (PMA). The CMPs can be readily and stably granulated by a ball-milling and sonication process, and then incorporated in 1,2-dioxetane cross-linked PMA to reinforce the polymer films, whose failure process can be characterized vividly by mechanochemiluminescent events. Moreover, the fluorescent CMP fillers also acted as energy acceptors during the tensile process of the composites, so that their prominent optical properties can be translated into the composite materials to improve the emission sensitivity (Scheme 1B). For the first time, the dual responses of granulated CMPs regarding their mechanical and optical properties in polymer nanocomposites were well demonstrated at a molecular level through chemiluminescent events, highlighting the enormous capabilities of CMPs to construct high-performance polymeric materials whose failure details can be self-reported sensitively.

Experimental

Preparation of granulated CMPs

The fluorescent **TPE-CMP** and **TPA-CMP** were synthesized according to the literature.[25] CMPs (120 mg) were wet ball-milled with DMF (5 mL) as a medium at 300 rpm for 20 h; the process was stopped for 5 min every 30 min. The obtained CMP suspensions were diluted with THF to 30 mL, and the concentration of CMP suspensions was 4 mg mL^{-1}. Then the suspensions were sonicated for 30 min and homo-dispersive CMPs were obtained.

General preparation process of CMP/PMA composite films

200 mg of linear PMA and granulated CMP suspension were stirred at 55 °C for 6 h, and linear PMA acted as a stabilizer of the granulated CMPs in THF. The mechanophore cross-linker (10 mg), 2,2′-azobis(2-methylpropionitrile) (AIBN, 20 mg) and methyl acrylate (MA, 2.0 mL) were put into the above suspensions and stirred until there was homo-dispersion, and then purged with argon. The polymerizations were conducted in a glove box, and the reaction mixtures were put into Teflon moulds (45 × 25 × 10 mm) with a glass pane above to prevent rapid evaporation of MA and THF. The Teflon moulds with the reaction mixtures were heated at 55 °C for 12 h and the composite films were obtained. The samples were dried in a vacuum at room temperature for 48 h, and weighed to calculate weight fractions ω (%) of CMPs in the polymer composites.

$$\omega = \frac{m'}{m} \times 100\%$$

where m' (g) is the weight of granulated CMPs and can be calculated by the volume and concentration of CMP suspensions, and m (g) is the weight of the composite films after drying.

Optomechanical testing

Tensile experiments were carried out on a TA Rheometrics, DHR-2 equipped with an Xpansion Instruments, SER3, extensional fixture. The drums of the fixture are colored black with a permanent marker to eliminate reflecting light. Transparent double-sided sticky tape was put on the drums to tightly fix the polymer film without slippage. A pco.edge 5.5 camera equipped with a Nikon AF NIKKOR 50 mm 1 : 1.4D lens was used to record videos in the dark. All of the videos were recorded in the rolling shutter color mode with a shooting rate of 200 fps and an exposure time of 5.0 ms. The frames of the resulting video were exported as separate monochrome TIF-files and light intensity was analyzed with a homemade program in MATLAB as in the literature.[19] The total intensity for a dark image as the noisy signal was subtracted from all film intensities.

Results and discussion

The chemical structures of CMPs (**TPE-CMP** and **TPA-CMP**) are shown in Fig. 1. They were selected to prepare dispersed nano-fillers owing to their unique optical properties. Both of the CMPs are highly fluorescent and exhibit strong absorption at 420 nm, and might potentially serve as fluorescent acceptors of the excited adamantyl ketone (λ_{em} = 420 nm). **TPE-CMP** and **TPA-CMP** could be facilely synthesized according to the literature[25] *via* Knoevenagel reactions of 1,4-phenylenediacetonitrile and 4-formylphenyltetraphenylethene or 4,4′,4″-triformyltriphenylamine. In contrast to other porous polymers, the presence of strong covalent bonds in CMPs provides sufficient

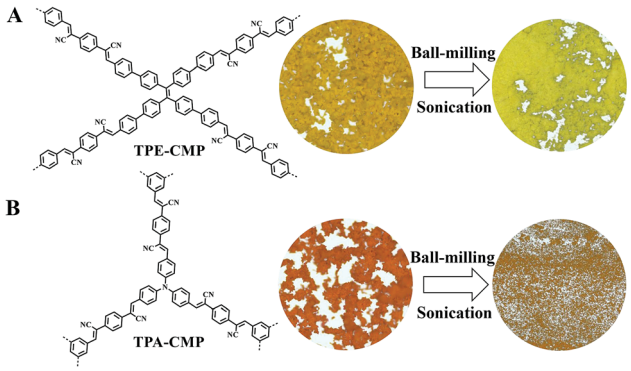

Fig. 1 (A) Structures and microscopic images of TPE-CMP. (B) Structures and microscopic images of TPA-CMP.

opportunities to obtain stable nano-structures. Herein, mechanical treatment, through ball-milling and sonication procedures, was employed as a facile and scalable approach to prepare granulated **TPE-CMP** and **TPA-CMP**.

Due to the good thermal and chemical stability of **TPE-CMP** and **TPA-CMP**, both the granulated CMPs retained their chemical structure throughout the mechanical process, as confirmed by the unchanged FT-IR spectra and solid state NMR (Fig. S3 and S4†). The thermal gravimetric analysis (TGA) curves showed that the good thermostability of granulated CMPs was well maintained (Fig. S5†). According to powder X-ray diffraction (XRD) profiles, the granulated CMPs were amorphous, like the as-synthesized samples, since no distinctive diffraction peaks were detected (Fig. S6†). Nitrogen adsorption/desorption experiments were performed to check the effect of surface area upon mechanical treatment (Fig. S7†). The isotherms of the granulated CMPs displayed drastically decreased surface areas, which has also been observed in other delamination cases for porous materials, and could be ascribed to the destroyed microporous structures when subjected to a strong mechanical force.[26,27]

The morphologies of the CMPs changed obviously after dispersion. The microscopic images showed that the macro-morphologies of pristine **TPE-CMP** and **TPA-CMP** were amorphous particles with a mustard and orange color, respectively. After processing with ball-milling followed by sonication, the granulated **TPE-CMP** appeared as compact sheets with a lemon yellow color. While the granulated **TPA-CMP** showed a finely ground morphology and its orange color did not change markedly (Fig. 1 and S8†). Scanning electron microscopy (SEM, Fig. S9†) images further revealed that the morphology of **TPE-CMP** transformed from amorphous particles to a compact flaky structure; meanwhile, spherical particles of **TPA-CMP** turned into nano-sheets with a much smaller size after granulation. According to the high resolution transmission electron microscopy (TEM) images (Fig. S10†), both CMPs and granulated CMPs had homogenous textures. Combined with atomic force microscope (AFM) analysis, **TPE-CMP** and granulated **TPE-CMP** were both flaky structures, while **TPA-CMP** and granulated **TPA-CMP** were irregular shapes, indicating the different architectural rigidities of **TPE-CMP** and **TPA-CMP**. The thickness of the two granulated CMPs were much thinner than the as-synthesized **TPE-CMP** and **TPA-CMP**, revealing that the CMPs were granulated successfully by mechanical processing (Fig. S11 and S12†).

The optophysical properties of the granulated CMPs were assessed by UV-Vis absorption and fluorescence spectra (Fig. 2). Similar to bulky CMPs, both the granulated CMPs exhibited strong absorption at 420 nm, allowing efficient energy transfer from emissive broken 1,2-dioxetane to these granulated CMP acceptors. When excited with 420 nm light, the fluorescence spectra of granulated **TPE-CMP** and **TPA-CMP** displayed bright fluorescence with emission colors of yellow and orange, respectively. The emission maximum for granulated **TPE-CMP** shifted hypochromically by *ca.* 43 nm compared with that of pristine **TPE-CMP**, while the emission peak for granulated **TPA-CMP** did not shift upon mechanical procedures. Such optical variation was reasonable, since the TPE moiety possessed a more rigid skeleton than TPA; therefore, at the molecular level, the conjugated degree of **TPE-CMP** could be influenced more prominently. Notably, comparison of the fluorescence quantum yields of the CMPs and granulated CMPs showed that they had similar values (Φ_f for **TPE-CMP**: 16.6%, **TPA-CMP**: 4.4%, granulated **TPE-CMP**: 22.9%, granulated **TPA-CMP**: 3.9%, Table S2†), which is critical for their utility as fluorescent acceptors. From the results of microporosity loss, changing morphology and the blue shift of emission, the granulated CMPs might show weakened π–π stacking[15,27] and decreased polymerization degrees[28,29] compared with those before granulation.

Given the good stability and fluorescent properties of these granulated CMPs, we further explored their applications as dual-functional nano-fillers. To fabricate reinforced mechano-luminescent polymer nanocomposites, the granulated CMPs suspensions were firstly stabilized by a small amount of linear PMA with various feed ratios. Cross-linked PMA with 1,2-dioxetane mechanophore as the cross-linker were then synthesized as the elastic matrix in the presence of the stabilized nanosheets (see ESI†). The components of all the composite films are illustrated in Tables 1 and S1.† It was inferred from the FT-IR spectra (Fig. S13†) and TGA curves (Fig. S14†) that the chemical structures and thermostability of the PMA matrix have not been changed in the composite films. DSC curves of all the films

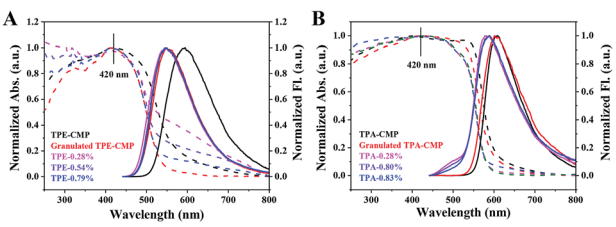

Fig. 2 UV-Vis spectra (dashed) and fluorescence spectra (solid) of (A) TPE-CMP, granulated TPE-CMP and TPE-CMP/PMA composite films; (B) TPA-CMP, granulated TPA-CMP and TPA-CMP/PMA composite films.

Table 1 The composition ratios of blank PMA and CMP/PMA composite films

	Linear PMA (mg)	Granulated CMP (mg)	MP (mg)	MA (mL)	Weight fraction of CMP
Blank	200	0	10	2.0	0
TPE-0.28%	200	2	10	2.0	0.28%
TPE-0.54%	200	4	10	2.0	0.54%
TPE-0.79%	200	6	10	2.0	0.79%
TPA-0.28%	200	2	10	2.0	0.28%
TPA-0.80%	200	4	10	2.0	0.80%
TPA-0.83%	200	6	10	2.0	0.83%

(Fig. S15†) demonstrated their elastic nature with a glass transition temperature (T_g) in the range of 11–19 °C, which would be favorable for the efficient conduction of mechanical force through the polymer chains. Fig. S16† depicts the CMP/PMA the composite films by SEM. The surface of the blank PMA films was homogeneous, while in the composite films, the nanoscale sheets in the marked areas may be nanosized CMPs which were pulled out of the matrix[15] morphologies of the fracture surfaces of blank PMA. There is no obvious agglomeration of CMP nanostructures, indicating good dispersion of these nano-fillers in PMA.

All the CMP/PMA composite films exhibited strong absorption at 420 nm, and emitted bright luminescence when excited at 420 nm (Fig. 2), demonstrating the positive role of CMP nanosheets in manifesting the optical performance of the composite films. Compared with granulated **TPE-CMP**, the **TPE-CMP/PMA** composite films presented similar UV-Vis absorption and fluorescence emission, while the **TPA-CMP/PMA** composite films exhibited a blue-shift in both UV-Vis absorption and fluorescence spectra compared with the granulated **TPA-CMP**. These results reflected the different diluting effects of the nano-fillers by PMA chains; that is, less influence was detected from **TPE-CMP** due to its compact flaky structure while the more flexible and finely powdered structure of granulated **TPA-CMP** could be further dispersed within the polymer media.

Optomechanical tests of blank PMA and CMP/PMA composites were then carried out on a rheometer equipped with two rotating drums, which allowed for uniform extensional deformation, to facilitate luminescence recording with a high-speed camera (see ESI, Fig. S18†). As illustrated in Videos S1–S3,† upon deformation, increased luminescence intensity combined with a pronounced localization of scission at the location of the fracture was observed, corresponding to activation of the 1,2-dioxetane group. Under the same conditions as for controlled composite films without covalently linked 1,2-dioxetane, no light was detected, confirming the mechanochemical nature of the luminescence.

Within 1,2-dioxetane as the luminescent force probe, sensitive tracing of the fracture process and quantitative characterization of the mechanical strength for different films were possible, by following their stress *vs.* strain and stress *vs.* light intensity curves simultaneously. Since the enhancement effect of nanomaterials on the polymer matrix was very sensitive to the amount of nano-fillers, optimized weight percentages of CMP nanosheets were then screened. As shown in Fig. 3A, the rupture stress and the elongation at break of the **TPE-CMP/PMA** composites increased obviously compared with those of blank PMA. For instance, among the three composite films, the one containing 0.28 wt% **TPE-CMP** exhibited the largest fracture strength, with an increment by about 105%. Further adding **TPE-CMP** nanosheets contributed a lot to the toughness of the as-prepared films, with elongation at break increasing by about 5% and 9% for TPE-0.54% and TPE-0.79%, respectively. Similar phenomena occurred in **TPA-CMP** containing composites (Fig. 3B), with either an improvement in rupture stress (eg, increasing by *ca.* 101% for TPA-0.28%) or rupture strain (eg, increasing by *ca.* 12% for TPA-0.83%) when the **TPA-CMP** contents were enhanced from 0.28% to 0.83%. Among the three samples, the most significant reinforcing effect from TPE-0.28% and TPA-0.28% was most probably correlated with their better particle dispersity in the polymer matrix (Fig. S17†). Compared to blank PMA, the efficiently enhanced mechanical properties of these polymer composites could be attributed to good

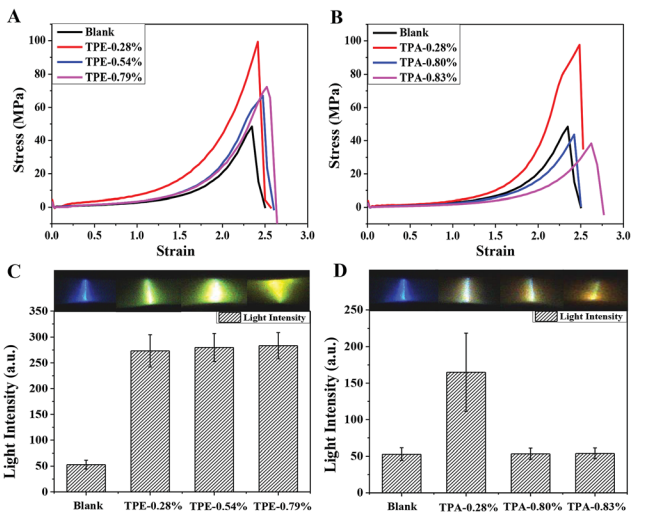

Fig. 3 Optomechanical test of TPE-CMP/PMA and TPA-CMP/PMA. (A) Typical stress–strain curves of blank PMA and TPE-CMP/PMA composites. (B) Typical stress–strain curves of blank PMA and TPA-CMP/PMA composites. (C) Total light intensity upon straining of blank PMA film and TPE-CMP/PMA composite films (above is an original picture of TPE-CMP/PMA at fracture). (D) Total light intensity upon straining of blank PMA film and TPA-CMP/PMA composite films (above is an original picture of TPA-CMP/PMA at fracture).

compatibility between the hydrophobic CMP surfaces and the PMA matrix.

Meanwhile, mechanically induced luminescence from these polymer films during fracture was quantified. Analysis of the representative videos taken from the deformation process of **TPE-CMP/PMA** and **TPA-CMP/PMA** composites demonstrated good temporal and spatial resolutions of mechanoluminescence (Videos S1–S3,† Fig. 3C and D). Assuming that integrated light intensity is proportional to the number of dioxetane scission events, the summed intensities of all frames up to a certain time is thus a measure of the total number of broken 1,2-dioxetane bonds up to that moment.[21] As illustrated in Fig. 4, when the cumulated light intensities are plotted against the applied strain, similar viscoelastic behavior, compared to the stress–strain curves, is observed (Fig. 4 and S19†). Relative to blank PMA without nanoscaled additives, the light intensity of all the **TPE-CMP/PMA** composites was enhanced greatly, as it is 400% higher than that of the blue emission from neat PMA (Fig. 3C). Such an observation could be attributed to the reinforcement effect of the composites on the mechanical stress, together with the efficient energy transfer process from broken 1,2-dioxetane emission to highly fluorescent **TPE-CMP**. Whereas for TPE-0.54% and TPE-0.79% with different values of mechanical strength, their similar light intensity could result from the competition between reduced stress and an increased amount of energy acceptor. As for **TPA-CMP/PMA**, TPA-0.28% with its distinguished improved mechanical performance also exhibited the most prominent mechanoluminescence, with an cumulated light intensity during stretching 200% higher than that of the neat PMA film. And, owing to the limited mechanical stress and quantum efficiency of **TPA-CMP**, the light intensities from TPA-0.80% and TPA-0.83% were almost the same as the unfilled PMA (Fig. 3D). Notably, the light colors from these polymer films could be readily tuned by adjusting the loading of CMP nanosheets, ranging from blue to orange with energy transfer. In other words, by carefully choosing the sorts and contents of granulated CMPs, fruitful optical properties controlled by mechanical force could be available, which would be important for fulfilling the needs of diverse applications.

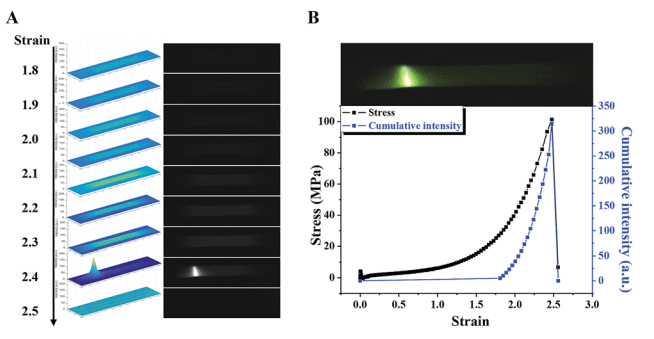

Fig. 4 Optomechanical test of TPE-0.28% in time and space. (A) Monochromatic optical images and intensity analysis of a bulk film of TPE-0.28% during stretching at a strain rate of 8 s^{-1}. (B) Diagram of stress and light intensity *vs.* strain of TPE-0.28% (above is an original picture of TPE-0.28% at fracture).

Conclusions

In this work, we presented a feasible strategy to fabricate mechanochemiluminescent polymer composites, by integrating CMP nano-fillers into 1,2-dioxetane cross-linked PMA. Two fluorescent CMPs nanosheets were prepared using a simple and economically friendly mechanochemical approach. Benefiting enormously from their polymer characteristics, these nano materials can be well dispersed and incorporated into a PMA matrix with good stability and compatibility. The granulated fluorescent CMPs served not only as nano-fillers to reinforce the mechanical properties of the resulting polymers, but also as fluorescent acceptors to improve light intensity with adjustable energy transfer efficiency. Imparted with the exceptional features of a 1,2-dioxetane based force probe, mechanically induced chemiluminescence with higher sensitivity and tunable emission colors was realized from this new kind of filling-type polymer nanocomposite, enabling the study of bond scission events in polymer nanocomposites with high sensitivity and resolution in space and time. We anticipate that, beyond the currently used CMPs, introducing proper fluorescent nano-fillers into mechanochemiluminescent polymers could be developed as a universal method to enhance both mechanical properties and emission sensitivities. This work thus not only provides guidance for broadening the application of CMP materials into nanocomposites, but also opens up a new avenue to investigate the failure mechanism of polymer nanocomposites at a molecular level.

Conflicts of interest

The authors declare no conflict of interest.

Acknowledgements

Financial support by the National Natural Science Foundation of China (Grants 21522405, 51503142 and 21734006), the National Key Research and Development Program of China (Grants 2017YFA0204503 and 2017YFA0207800), the Thousand Youth Talents Plan and the Natural Science Foundation of Tianjin (Grants 15JCYBJC52900 and 17JCJQJC44200) is gratefully acknowledged.

Notes and references

1 S. C. Tjong, *Mater. Sci. Eng., R*, 2006, **53**, 73–197.
2 S.-Y. Fu, X.-Q. Feng, B. Lauke and Y.-W. Mai, *Composites, Part B*, 2008, **39**, 933–961.
3 B. T. McGrail, A. Sehirlioglu and E. Pentzer, *Angew. Chem., Int. Ed.*, 2015, **54**, 1710–1723.
4 S. K. Kumar, B. C. Benicewicz, R. A. Vaia and K. I. Winey, *Macromolecules*, 2017, **50**, 714–731.
5 S. J. Eichhorn, A. Dufresne, M. Aranguren, N. E. Marcovich, J. R. Capadona, S. J. Rowan, C. Weder, W. Thielemans, M. Roman, S. Renneckar, W. Gindl, S. Veigel, J. Keckes, H. Yano, K. Abe, M. Nogi, A. N. Nakagaito, A. Mangalam,

J. Simonsen, A. S. Benight, A. Bismarck, L. A. Berglund and T. Peijs, *J. Mater. Sci.*, 2010, **45**, 1–33.

6 N. Huang, P. Wang and D. Jiang, *Nat. Rev. Mater.*, 2016, **1**, 16068.

7 G. Das, B. P. Biswal, S. Kandambeth, V. Venkatesh, G. Kaur, M. Addicoat, T. Heine, S. Verma and R. Banerjee, *Chem. Sci.*, 2015, **6**, 3931–3939.

8 I. Berlanga, R. Mas-Balleste and F. Zamora, *Chem. Commun.*, 2012, **48**, 7976–7978.

9 I. Berlanga, M. L. Ruiz-Gonzalez, J. M. Gonzalez-Calbet, J. L. Fierro, R. Mas-Balleste and F. Zamora, *Small*, 2011, **7**, 1207–1211.

10 D. N. Bunck and W. R. Dichtel, *J. Am. Chem. Soc.*, 2013, **135**, 14952–14955.

11 A. Belen Marco, D. Cortizo-Lacalle, I. Perez-Miqueo, G. Valenti, A. Boni, J. Plas, K. Strutynski, S. De Feyter, F. Paolucci, M. Montes, A. N. Khlobystov, M. Melle-Franco and A. Mateo-Alonso, *Angew. Chem., Int. Ed.*, 2017, **56**, 6946–6951.

12 J. Dechnik, J. Gascon, C. J. Doonan, C. Janiak and C. J. Sumby, *Angew. Chem., Int. Ed.*, 2017, **56**, 9292–9310.

13 H. Vinh-Thang and S. Kaliaguine, *Chem. Rev.*, 2013, **113**, 4980–5028.

14 K. Wu, J. Guo and C. Wang, *Angew. Chem., Int. Ed.*, 2016, **55**, 6013–6017.

15 X. Mu, J. Zhan, X. Feng, B. Yuan, S. Qiu, L. Song and Y. Hu, *ACS Appl. Mater. Interfaces*, 2017, **9**, 23017–23026.

16 Z. Xiang, H. Sun, Z. Zhu, W. Liang, B. Yang and A. Li, *RSC Adv.*, 2015, **5**, 24893–24898.

17 D. A. Davis, A. Hamilton, J. Yang, L. D. Cremar, D. Van Gough, S. L. Potisek, M. T. Ong, P. V. Braun, T. J. Martinez, S. R. White, J. S. Moore and N. R. Sottos, *Nature*, 2009, **459**, 68–72.

18 S. Garcia-Manyes and A. E. M. Beedle, *Nat. Rev. Chem.*, 2017, **1**, 16.

19 Y. Chen, A. J. Spiering, S. Karthikeyan, G. W. Peters, E. W. Meijer and R. P. Sijbesma, *Nat. Chem.*, 2012, **4**, 559–562.

20 E. Ducrot, Y. Chen, M. Bulters, R. P. Sijbesma and C. Creton, *Science*, 2014, **344**, 186–189.

21 Y. Chen and R. P. Sijbesma, *Macromolecules*, 2014, **47**, 3797–3805.

22 Z. S. Kean, J. L. Hawk, S. Lin, X. Zhao, R. P. Sijbesma and S. L. Craig, *Adv. Mater.*, 2014, **26**, 6013–6018.

23 J. M. Clough, J. van der Gucht and R. P. Sijbesma, *Macromolecules*, 2017, **50**, 2043–2053.

24 J. M. Clough, C. Creton, S. L. Craig and R. P. Sijbesma, *Adv. Funct. Mater.*, 2016, **26**, 9063–9074.

25 Y. Wei, W. Chen, X. Zhao, S. Ding, S. Han and L. Chen, *Polym. Chem.*, 2016, **7**, 3983–3988.

26 K. S. W. Sing, D. H. Everett, R. A. W. Haul, L. Moscou, R. A. Pierotti, J. Rouquerol and T. Siemieniewska, *Pure Appl. Chem.*, 1985, **57**, 603.

27 S. Chandra, S. Kandambeth, B. P. Biswal, B. Lukose, S. M. Kunjir, M. Chaudhary, R. Babarao, T. Heine and R. Banerjee, *J. Am. Chem. Soc.*, 2013, **135**, 17853–17861.

28 Y. Xu, L. Chen, Z. Guo, A. Nagai and D. Jiang, *J. Am. Chem. Soc.*, 2011, **133**, 17622–17625.

29 F. Delogu, G. Gorrasi and A. Sorrentino, *Prog. Mater. Sci.*, 2017, **86**, 75–126.